Direct Transition from Quantum Escape to a Phase Diffusion Regime in YBaCuO Biepitaxial Josephson Junctions

Luigi Longobardi,[1,2,*] Davide Massarotti,[2,3] Daniela Stornaiuolo,[2] Luca Galletti,[2,3] Giacomo Rotoli,[1] Floriana Lombardi,[4] and Francesco Tafuri[1,2]

[1]Seconda Universitá degli Studi di Napoli, Dipartimento di Ingegneria dell'Informazione, via Roma 29, I-81031 Aversa (Ce) Italy
[2]CNR-SPIN UOS Napoli, Complesso Universitario di Monte Sant'Angelo via Cinthia, I-80126 Napoli (Na) Italy
[3]Universitá degli Studi di Napoli Federico II, Dipartimento di Scienze Fisiche, via Cinthia, I-80126 Napoli (Na) Italy
[4]Department of Microtechnology and Nanoscience, Chalmers University of Technology, S-41296 Göteborg, Sweden

(Received 23 January 2012; published 1 August 2012; publisher error corrected 9 August 2012)

Dissipation encodes the interaction of a quantum system with the environment and regulates the activation regimes of a Brownian particle. We have engineered grain boundary biepitaxial YBaCuO junctions to drive a direct transition from a quantum activated running state to a phase diffusion regime. The crossover to the quantum regime is tuned by the magnetic field and dissipation is described by a fully consistent set of junction parameters. To unravel phase dynamics in moderately damped systems is of general interest for advances in the comprehension of retrapping phenomena and in view of quantum hybrid technology.

DOI: 10.1103/PhysRevLett.109.050601 PACS numbers: 05.40.Jc, 74.50.+r, 85.25.Cp

The remarkable development of superconductive systems in the field of quantum information processing and the expertise gained on manipulating coherent entangled states and different coupling regimes with the environment [1] have boosted research on several complementary aspects of coherence and dissipation. Because of their design scalability and their flexibility in controlling the level of damping, Josephson systems have proven to be a fantastic test bench for studying fundamental physics problems such as the quantum superposition of alive and dead states of Schrödinger's cat [2], the behavior of an artificial atom in cavity quantum electrodynamics experiments [3], or measurements of quantum coherence in macroscopic systems [4,5].

Both the time evolution of the position of a Brownian particle and the electrodynamics of a Josephson junction (JJ) [6,7] can be described by a Langevin equation [8] of the form

$$\ddot{\varphi} + \dot{\varphi}/Q + dU/d\varphi = \xi(t). \quad (1)$$

In this equation, the time is normalized to $1/\omega_p$, with $\omega_p = (2eI_{co}/\hbar C)^{1/2}$ representing the plasma frequency at zero bias current I_{co} and C being the junction critical current in absence of thermal fluctuations and capacitance, respectively. The potential U is the well-known periodic "washboard" potential associated to the dynamic of a JJ, $U(\varphi) = -E_J(\cos\varphi + \frac{I}{I_{co}}\varphi)$, where $\varphi(t)$ is the superconductive phase and $E_J = \hbar I_{co}/2e$ is the Josephson energy. $\xi(t)$ is a white noise driving force such that

$$\langle \xi(t) \rangle = 0; \qquad \langle \xi(t), \xi(t') \rangle = \sqrt{k_B T/QE_J}\delta(t - t'). \quad (2)$$

The parameter Q is given by $Q = \omega_p RC$ [6,7] with R the shunt resistance. In a more general approach, Q has a frequency dependence [9] better responding to the need of including external shunting impedance. In our case, the simplest approach based on the Q factor calculated only at plasma frequency [10,11], gives a satisfying account for experimental data, as demonstrated below. It is a natural choice to use a JJ in order to study the Brownian motion of a particle in a dissipative tilted periodic potential [see Figs. 1(a) and 1(b)].

In this Letter, we demonstrate a direct transition from a running state, obtained following a quantum activation, to diffusive Brownian motion in YBaCuO JJs. Multiple retrapping processes in subsequent potential wells characterize phase regimes where diffusive phenomena play a relevant role [9–13] [see Fig. 1(b)]. The relevant parameters driving the occurrence of these phenomena are the operational temperature T, the damping factor Q, and the critical current I_{co}. The various operation scenarios for a JJ have been condensed in a phase diagram by Kivioja *et al.* [10] who have shown that by spanning the $(E_J, k_B T)$ parameter space it is possible to engineer all different regimes ranging from phase diffusion (PD) and thermal activation (TA) to macroscopic quantum tunneling (MQT). MQT takes place not only for low values of dissipation ($Q \gg 1$), but also for intermediate levels of dissipation ($1 < Q < 5$). We explore a new region of this phase diagram, made available by the different ranges of I_{co} and of the standard deviation of the switching distribution σ offered by these junctions when compared with most low temperature superconductor JJs. The moderately damped systems are particularly significant and promising to address and quantify interactions of a quantum system with the environment [14] which is, apart from the its intrinsic interest for fundamental physics, a cornerstone for the development of whatever quantum hybrid technology.

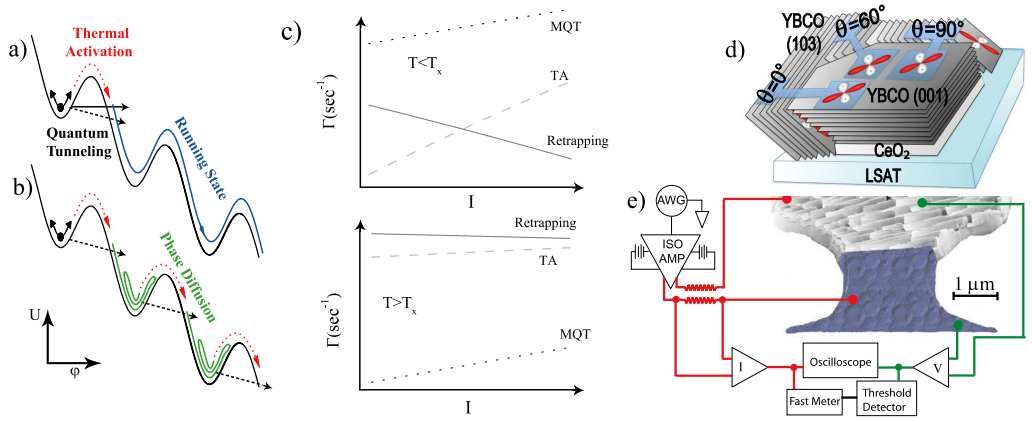

FIG. 1 (color online). (a) Thermal (red dashed line) or quantum activated escape in the tilted periodic potential. Quantum escape is represented for both very low ideal ($Q \gg 1$, continuous black line) and high ($1 < Q < 5$, dashed black line) levels of dissipation, respectively. (b) Diffusive motion due to multiple escapes and retrapping in subsequent potential wells. (c) Schematic escape rates of MQT, TA, and retrapping processes at $T < T_x$ (top panel) and $T > T_x$ (bottom panel). (d) Sketch of the off-axis biepitaxial junctions. The JJ is formed at the boundary between (001) YBaCuO and (103) YBaCuO electrodes. Three interface orientations $\theta = 0°$, 60°, and 90° are shown as examples. Different interface orientations (lobe vs lobe, node vs lobe, and any configuration in between) can be achieved with proper patterning of the seed layer [23]. (e) Picture of the device along with a block diagram of the experimental setup. In the bottom part of the image (in blue) is the YBaCuO (001) electrode while in the top part (gray) the needlelike YBaCuO (103) grains are visible.

The experimental observation of the various phase dynamics regimes in a JJ is based on the measurement of the switching current distribution (SCD) and the study of the behavior of its first and second momenta (the mean $\bar{I}$ and the width σ) as function of temperature. In an underdamped junction ($Q > 10$) [15], below a crossover temperature T_x the escape process is mostly due to MQT [see Fig. 1(a)], marked by a temperature-independent σ, while above T_x the process of escape is due to TA above the potential barrier, with a distinctive increase of σ with temperature. In moderately damped junctions [9–11,13,16–18] with $2 < Q < 5$, a transition from TA to PD regime occurs at a crossover temperature $T^* > T_x$. T^* marks a distinctive change in the sign of the temperature derivative of σ, with $d\sigma/dT > 0$ for $T < T^*$ and $d\sigma/dT < 0$ for $T > T^*$. When escape out of a well occurs at too low currents in PD regime [9], the energy gained by passing from one well to the next one barely exceeds the dissipative losses and the particle eventually gets retrapped. In this diffusive regime, the SCD histograms move to lower currents I till they touch the limit value $I_R = (4 \times I_{co}/\pi)1/Q$ in the most common cases with $Q \gg 1$ [9,19].

We report measurements of SCD in a temperature range from 20 mK to 2.2 K. Our data are characterized by two distinct regimes. Below 135 mK the widths of the SCDs show no significative variation. This is a typical signature of a quantum activation regime. Above 135 mK the negative temperature derivative of σ is consistent with a diffusive motion due to multiple retrapping in the potential wells. This regime has been fitted using existing theories on PD [18] with a damping factor $Q = 1.3$. The observations are qualitatively consistent with the escape rates sketched in Fig. 1(c). We have substantially engineered a device with $T^* \lesssim T_x$. For temperatures T well below T_x, MQT contributions to escape rates are larger than those coming from both thermal escape and multiple retrapping processes [Fig. 1(c), top panel], which is different from the case $T > T_x$ [Fig. 1(c), bottom panel]. The contiguity between quantum escape ($T < T_x$) and PD ($T > T_x$) leads to MQT phenomena characterized by low Q values and not necessarily to quantum PD. This MQT process can be represented in Fig. 1(a) as a dashed line to manifest interaction with the environment [20], and responds to what it can be possibly experimentally ascertained. This phenomenology is quite distinct from all previous studies [9–11,13,16–18], where in the transition to quantum activation, retrapping processes decay faster than thermal escape, and from the work of Yu *et al.* [21], where the occurrence of a quantum activated PD has been claimed. In Ref. [21], the semiclassical nature of their quantum PD is testified by the dependence of σ on the temperature over the entire temperature range, and the transition is as a matter of fact revealed by a change of the temperature derivative of σ [21]. MQT processes are substantially followed and assisted by thermally ruled retrapping processes. However, a fully quantum account of phase fluctuations passes through the "empirical" condition of a Josephson energy much larger than Coulomb energy, $E_J \gg E_C$ with $E_C = e^2/2C$ (see below), given by Iansiti *et al.* [22]. This condition does not occur both in the present experiment and in the work of Yu *et al.* [21], both of which represent complementary significant advances toward the observation of a fully

quantum PD, better defining its domain and the border with competing processes.

We have used YBaCuO off-axis grain boundary (GB) biepitaxial JJs, whose scheme is shown in Fig. 1(d) [23–25]. The GB is determined at the boundary between the 103-oriented grains growing on the bare substrate and the 001 grain growing on the CeO_2 seed layer. We have engineered junctions on $(La_{0.3}Sr_{0.7})(Al_{0.65}Ta_{0.35})O_3$ (LSAT) rather than on $SrTiO_3$ (STO) substrates, where MQT in a high temperature superconductor JJ was first demonstrated [25]. The new design fully responds to the need of reducing stray capacitances and isolating the GB behavior [26]. Specific capacitances are one order of magnitude lower than those measured on STO-based devices [25,26]. Dynamical junction parameters can be tuned by choosing the interface orientation indicated by the angle θ in Fig. 1(d), which also sets d-wave induced effects [23,24].

To study the escape rates of YBaCuO JJs, we have thermally anchored the sample to the mixing chamber of a He3/He4 Oxford dilution refrigerator and performed measurements of the junction switching current probability. A schematic representation of our experimental setup is shown in Fig. 1(e). A full description of the apparatus is discussed in detail elsewhere [17]. Filtering is guaranteed by a room temperature electromagnetic interference filter stage followed by low pass RC filters with a cutoff frequency of 1.6 MHz anchored at 1.5 K, and by a combination of copper powder and twisted pair filters thermally anchored at the mixing chamber of the dilution refrigerator. The bias current of the junction is ramped at a constant sweep rate $dI/dt = 17.5\ \mu$A/s and at least 10^4 switching events have been recorded using a standard technique. These measurements, collected over a wide range of temperatures, are reported in Fig. 2(a). A progressive broadening of the histograms occurs when lowering the temperature, which is a distinctive feature of the PD regime [10,11,13,16–18]. For temperatures below about 135 mK, the histograms overlap.

The temperature dependence of the width σ of the SCD curves is shown in Fig. 2(b). As a test of fidelity for our fabrication process and our experimental setup, we report data for two different samples with interface orientations of 75° for sample A and 50° for sample B. The junctions are 2.5 and 2.0 μm wide, respectively, and the film thicknesses are 100 and 250 nm, respectively. We have selected interface orientations with robust overlap of the d-wave lobes on both sides of the junctions [24] and E_J of the order of 3 meV. For both samples above a temperature T^*, the data display a decrease in the width of the distribution in agreement with a process of multiple escapes and retrapping typical of the diffusive motion. The high temperature region (135 mK $< T <$ 2 K) allows a reliable estimation of the damping parameter. Simulations for $Q = 1.30$ are reported as a red line in Fig. 2(b) resulting from the integration of the Langevin Eq. (1) with a noise affected Bulirsh-Stoer integrator using Cernlib routine RANLUX [17].

In Fig. 2(c), simulated thermal behavior of σ is reported for different values of the Q damping parameter ranging from 1.2 to 5. For each of these curves, T^* approximately indicates the transition temperature from TA to the diffusive regime. Q tunes T^* as shown in the inset of Fig. 2(c) and modifies the slope of the $\sigma(T)$ falloff at higher temperatures. The capability to numerically reproduce this region makes it possible to estimate Q with high precision. In our case $Q = 1.30 \pm 0.05$ closely fits the data and determines a T^* value not larger than 100 mK. The section below T^* faithfully reproduces the expected

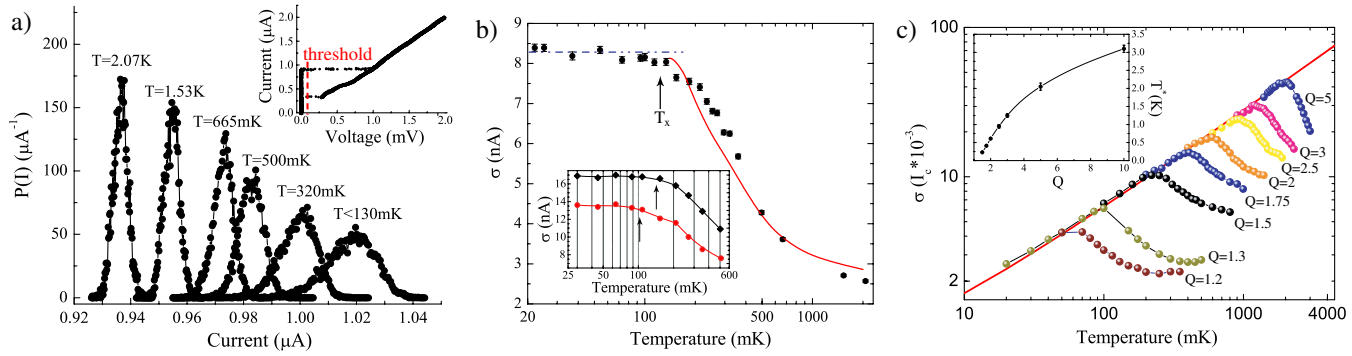

FIG. 2 (color online). (a) Measured switching current probability distribution $P(I)$ at different bath temperatures, for sample A. The inset shows the device current voltage characteristic measured at 30 mK. The reference value for the threshold detector is also displayed. (b) Temperature dependence of the standard deviation, σ, of the switching distributions for sample A. The dash-dotted line marks the temperature-independent SCD widths in the quantum tunneling regime, the red solid line is the result of simulations in the diffusive regime with a damping parameter of $Q = 1.3$. The inset shows temperature dependent data for sample B acquired at two different values of the applied magnetic field. (c) Simulated thermal behavior of the width of the switching histogram for several values of the Q damping parameter. In the inset we report the dependence of the turn-over temperature T^* on the damping parameter.

TABLE I. Device parameters.

Sample	H (G)	I_{co} (μA)	R (Ω)	C (fF)	Q	T_x (mK)
A	0	1.20	84	64	1.30	135
B	0	1.79	64	74	1.28	144
B	12	1.42	64	74	1.14	122

$T^{2/3}$ dependence for a thermally activated regime [27] (solid line) as an additional test of consistency. In Fig. 2 (c), the MQT section is missing. It would attach below T_x to each of the curves with its characteristic saturation in σ, as shown in Fig. 2(b) in fitting experimental data.

Indeed below 135 mK, the experimental values of σ are almost independent of temperature and consistent with an escape dominated by quantum tunneling. Thus 135 ± 10 mK represents the crossover temperature T_x which, along with the value of Q previously extrapolated, allows us to determine the values of the capacitance $C = 64$ fF and of the plasma frequency $\omega_p \simeq 38$ GHz. This value of the capacitance C is also in agreement with the value extrapolated using the estimated specific capacitance $C_s \simeq 2 \times 10^{-5}$ F cm^{-2} for YBaCuO BP JJs on LSAT substrates [24,26]. As a consequence, $E_J \simeq 3$ meV results to be much larger than $E_C \simeq 3\,\mu$eV ($E_J/E_C \simeq 1000$) and the system is in conditions nominally far from those which are considered to be favorable for the observation of quantum PD [22].

We used the magnetic field to tune the junction parameters and T_x *in situ*, in order to unambiguously prove MQT as the source of the saturation of σ below T_x [15]. In the inset of Fig. 2(b), we report the temperature dependence of σ measured for sample B at two different magnetic fields of 0 and 12 G, respectively. $H = 12$ G lowers the critical current I_{co} reducing at the same time the quantum crossover temperature. Relevant device parameters are summarized in Table I.

In Fig. 3 we report a (Q, k_BT/E_J) phase diagram, which summarizes the various activation regimes [10]. The transition curve between the PD regime and the running state following thermal (experimentally observed in [10,11,13,17]) or quantum (experimentally observed in this work) activation has been determined numerically by varying the damping factor Q as function of the ratio between the thermal energy and the Josephson energy. The filled circles are experimental data obtained by fitting the escape rates Γ as a function of the ratio between the barrier height and the escape energy, $u = \Delta U/k_BT_{\rm esc}$ [28] (shown in the inset of Fig. 3). The obtained values fall within the region of the diagram that displays a direct transition from PD to quantum activation. The escape rates have been calculated from the switching distributions using a standard procedure [29]. In the quantum activated regime, the switching distributions are asymmetric and skewed to the left, and Γ values all fall onto the same line, as it is the case for the reported data from $T = 30$ to

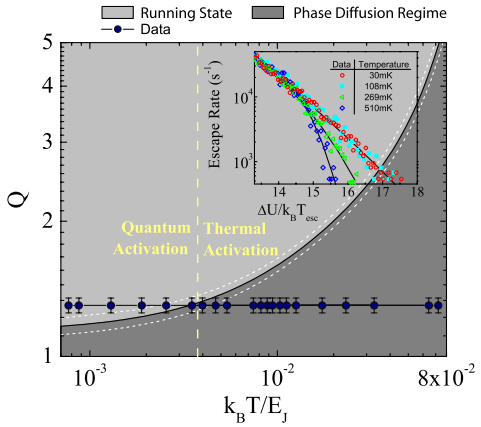

FIG. 3 (color online). (Q, k_BT/E_J) parameter space, showing the various activation regimes. The transition curve between the PD regime and the running state has been extrapolated through numerical simulations, the sideband curves mark the uncertainty in our calculation and are due to the temperature step size. The crossover temperature between the various regimes scales with E_J. The data points refer to the Q values of our sample and show the direct transition from quantum activated running state to the PD regime. In the inset we show the experimental escape rates (symbols) as function of barrier height to escape energy ratio along with the theoretical fits at different T. The Q values used for the fits are the same shown in the phase diagram.

108 mK. Retrapping processes cause a progressive symmetrization of the switching distribution which translates into a deviation of the experimental escape rates from the ideal exponential behavior [17,18].

In summary, by exploring a new region of the (Q, k_BT/E_J) phase diagram we have demonstrated a direct transition from quantum activation to diffusive Brownian motion in GB YBaCuO JJs. This experiment sets another milestone in the study of the influence of dissipation on the switching statistics of JJs [12,15,20,30–32] demonstrating novel balancing between MQT, thermally activated and retrapping escapes, thus paving the way to the observation of fully quantum PD, and is of particular relevance to understand interaction of a quantum system with the environment [14]. The combined experimental and numerical investigation here presented has the potential to offer a new tool to study the interplay between coherence phenomena and dissipation down to the quantum regime in a wide variety of systems.

We thank T. Bauch and A. Ustinov for stimulating discussions. Special gratitude to J. Clarke and A. J. Leggett for inspiring conversations. We thank A. J. Leggett again for a careful reading of the manuscript. We acknowledge financial support by EC MIDAS and by a Marie Curie Grant No. 248933 "hybMQC." We also acknowledge the support by MIUR-Italy through Prin-project 2009 "Nanowire high critical temperature superconductor field-effect devices" and by ISCRA the Italian

SuperComputing Resource Allocation through Grant No. IscrB_NDJJBS 2011. We have profited much from conversations with Professor Antonio Barone on the topics of this research.

*llongobardi@ms.cc.sunysb.edu

[1] J. Clarke and F. K. Wilhelm, Nature (London) **453**, 1031 (2008).

[2] J. R. Friedman, V. Patel, W. Chen, S. K. Tolpygo, and J. E. Lukens, Nature (London) **406**, 43 (2000).

[3] A. Wallraff, D. I. Schuster, A. Blais, L. Frunzio, R.-S. Huang, J. Majer, S. Kumar, S. M. Girvin, and R. J. Schoelkopf, Nature (London) **431**, 162 (2004).

[4] Y. Nakamura, Y. A. Pashkin, and J. S. Tsai, Nature (London) **398**, 786 (1999).

[5] I. Chiorescu, Y. Nakamura, C. J. P. M. Harmans, and J. E. Mooij, Science **299**, 1869 (2003).

[6] A. Barone and G. Paternò, *Physics and Applications of the Josephson Effect* (John Wiley & Sons, New York, 1982).

[7] K. K. Likharev, *Dynamics of Josephson Junctions and Circuits* (Gordon and Breach Science Publishers, New York, 1986).

[8] P. Langevin, C.R. Acad. Sci. Paris **146**, 530 (1908).

[9] R. L. Kautz and J. M. Martinis, Phys. Rev. B **42**, 9903 (1990); J. M. Martinis and R. L. Kautz, Phys. Rev. Lett. **63**, 1507 (1989).

[10] J. M. Kivioja, T. E. Nieminen, J. Claudon, O. Buisson, F. W. J. Hekking, and J. P. Pekola, Phys. Rev. Lett. **94**, 247002 (2005).

[11] J. Männik, S. Li, W. Qiu, W. Chen, V. Patel, S. Han, and J. E. Lukens, Phys. Rev. B **71**, 220509 (2005).

[12] D. Vion, M. Götz, P. Joyez, D. Esteve, and M. H. Devoret, Phys. Rev. Lett. **77**, 3435 (1996).

[13] V. M. Krasnov, T. Bauch, S. Intiso, E. Hürfeld, T. Akazaki, H. Takayanagi, and P. Delsing, Phys. Rev. Lett. **95**, 157002 (2005); V. M. Krasnov, T. Golod, T. Bauch, and P. Delsing, Phys. Rev. B **76**, 224517 (2007).

[14] A. O. Caldeira and A. J. Leggett, Phys. Rev. Lett. **46**, 211 (1981); A. O. Caldeira and A. J. Leggett, Ann. Phys. (N.Y.) **149**, 374 (1983).

[15] M. H. Devoret, J. M. Martinis, and J. Clarke, Phys. Rev. Lett. **55**, 1908 (1985); J. M. Martinis, M. H. Devoret, and J. Clarke, Phys. Rev. B **35**, 4682 (1987).

[16] M.-H. Bae, M. Sahu, H.-J. Lee, and A. Bezryadin, Phys. Rev. B **79**, 104509 (2009).

[17] L. Longobardi, D. Massarotti, G. Rotoli, D. Stornaiuolo, G. Papari, A. Kawakami, G. P. Pepe, A. Barone, and F. Tafuri, Phys. Rev. B **84**, 184504 (2011).

[18] J. C. Fenton and P. A. Warburton, Phys. Rev. B **78**, 054526 (2008).

[19] W. C. Stewart, Appl. Phys. Lett. **12**, 277 (1968).

[20] Yu. N. Ovchinnikov and A. Barone, J. Low Temp. Phys. **67**, 323 (1987); D. Waxman and A. J. Leggett, Phys. Rev. B **32**, 4450 (1985).

[21] H. F. Yu, X. B. Zhu, Z. H. Peng, Y. Tian, D. J. Cui, G. H. Chen, D. N. Zheng, X. N. Jing, L. Lu, S. P. Zhao, and S. Han, Phys. Rev. Lett. **107**, 067004 (2011).

[22] M. Iansiti, A. T. Johnson, W. F. Smith, H. Rogalla, C. J. Lobb, and M. Tinkham, Phys. Rev. Lett. **59**, 489 (1987); M. Iansiti, M. Tinkham, A. T. Johnson, W. F. Smith, and C. J. Lobb, Phys. Rev. B **39**, 6465 (1989).

[23] F. Lombardi, F. Tafuri, F. Ricci, F. M. Granozio, A. Barone, G. Testa, E. Sarnelli, J. R. Kirtley, and C. C. Tsuei, Phys. Rev. Lett. **89**, 207001 (2002).

[24] F. Tafuri and J. R. Kirtley, Rep. Prog. Phys. **68**, 2573 (2005).

[25] T. Bauch, F. Lombardi, F. Tafuri, A. Barone, G. Rotoli, P. Delsing, and T. Claeson, Phys. Rev. Lett. **94**, 087003 (2005); T. Bauch, T. Lindstrom, F. Tafuri, G. Rotoli, P. Delsing, T. Claeson, and F. Lombardi, Science **311**, 57 (2006).

[26] D. Stornaiuolo, G. Papari, N. Cennamo, F. Carillo, L. Longobardi, D. Massarotti, A. Barone, and F. Tafuri, Supercond. Sci. Technol. **24**, 045008 (2011).

[27] L. D. Jackel, J. P. Gordon, E. L. Hu, R. E. Howard, L. A. Fetter, D. M. Tennant, R. W. Epworth, and J. Kurkijarvi, Phys. Rev. Lett. **47**, 697 (1981); J. Kurkijärvi, Phys. Rev. B **6**, 832 (1972).

[28] There are two different definitions for the escape temperature T_{esc} based on the particle activation being dominated by quantum or thermal effects. For a more detailed explanation please refer to Devoret *et al.* [15].

[29] T. A. Fulton and L. N. Dunkleberger, Phys. Rev. B **9**, 4760 (1974).

[30] Y. C. Chen, M. P. A. Fischer, and A. J. Leggett, J. Appl. Phys. **64**, 3119 (1988).

[31] J. R. Kirtley, C. D. Tesche, W. J. Gallagher, A. W. Kleinsasser, R. L. Sandstrom, S. I. Raider, and M. P. A. Fisher, Phys. Rev. Lett. **61**, 2372 (1988).

[32] A. Barone, R. Cristiano, and P. Silvestrini, J. Appl. Phys. **58**, 3822 (1985); P. Silvestrini, S. Pagano, R. Cristiano, O. Liengme, and K. E. Gray, Phys. Rev. Lett. **60**, 844 (1988); M. G. Castellano, G. Torrioli, F. Chiarello, C. Cosmelli, and P. Carelli, J. Appl. Phys. **86**, 6405 (1999).